Review of Adhesion Fundamentals for Micron-Scale Particles†

Otis R. Walton
Grainflow Dynamics Inc.[1]

Abstract

The effects of various fundamental forces on the adhesion of fine dust particles are reviewed. The particle-size and distance variation of surface-energy related (e.g., van der Waals) forces are compared to similar relations for static-electric image-forces for tribo-charged particles near (or contacting) conducting surfaces. The van der Waals force (between macroscopic spheres), a patch-charge image-force and static-electric image-forces all exhibit an inverse square variation with distance; however, these forces have dramatically different ranges-of-effect. The very short-range nature of van der Waals forces (of order 10nm) is a major reason that most real contacts, involving non-smooth surfaces, exhibit adhesion forces that are substantially lower than values predicted for smooth particles. Based on studies of Lunar and Martian regolith stimulant powders, triboelectric charges on fine particles appear to scale linearly with particle size. It is shown that below some threshold size, the adhesion (to conducting surfaces) of charged dust particles possessing such a linear charge-to-size scaling relationship, may be dominated by image-charge forces, instead of surface-energy related interactions. This is counter to what might have been expected from a cursory examination of the fundamental force relations, which would suggest van der Waals adhesion forces would dominate for small particle sizes.

Keywords: adhesion, electrostatic, van der Waals attraction, fine Powder, image-charge force, dust

1. Introduction/Background

The effects of surface-energy and image-charge forces and how their relative strength varies with particle size and with distance was a major part of a recent NASA sponsored review of the potential effects of various fundamental forces acting on lunar dust particles [Walton, 2007]. Although primarily based on that NASA report, this paper attempts to de-emphasize special lunar conditions, like an ultra-high vacuum and high incident solar UV flux and solar wind effects, and instead, describes primarily those aspects of fine particle adhesion which are applicable under terrestrial conditions. Adhesion forces acting on fine particles can arise from a variety of causes including van der Waals (*i.e.*, surface energy) interactions, electrostatic interactions, static-electric image charges in nearby conductors, and, under high humidity conditions, surface tension in menisci of adsorbed water surrounding contact points. The effects of adsorbed water was not covered in the lunar dust review, since there is virtually no in-situ atmosphere on the moon and adsorbed water would likely only be a significant contribution to adhesion inside of human habitats. A perusal of the literature on the effects of humidity on particle-scale forces, however, indicates that for many particle/surface combinations there is a dramatic increase in adhesion at high humidities. The threshold value for this dramatic increase in adhesive force appears to depend relatively strongly on the degree of surface roughness near contact points with rougher surfaces requiring higher humidity before the threshold is observed. Rabinovich [2000] and Rabinovich *et al* [2002] hypothesized that the dramatic increase in cohesion/adhesion occurs when the thickness of a layer of adsorbed water is great enough for the liquid water to 'bridge' the gap between the near surfaces (over a height comparable to the surface roughness). A number of AFM studies of the effect of humidity on adhesive forces have been

† Accepted : July 2, 2008
[1] 1141 Catalina Drive, PMB-270, Livermore, CA 94550, USA
TEL: (925)447-4293 FAX: (925)449-9111
E-mail: walton@grainflow.com

ⓒ 2008 Hosokawa Powder Technology Foundation

consistent with the ideas of Rabinovich and Moudgil. A few have found that increasing humidity decreases adhesion; however, this appears to occur most often when the initial adhesion is electrostatic in nature, so that the humidity allows the charge to leak away from the contact area. On the other hand, under very low humidity conditions, charge leak-off rates are quite low and particles can maintain charges for long periods of time. This paper does not directly examine the effects of humidity on adhesion; however analytic models exist for the distance and particle-size scaling of liquid meniscus forces for contacting spheres [Lian et al, 1993; Xue, 2007].

Fine non-conducting particles are strongly affected by surface-energy related (*i.e.*, van der Waals) interactions and by electrostatic forces. In powder handling operations conductive materials, or thin partially-conductive coatings, are often utilized to minimize charge buildup, and thus reduce problems from static-electric attraction of fine particles to surfaces. Utilization of conductive coatings or conductive materials can minimize the attraction of uncharged fine particles to charged surface regions; however the use of conducting surfaces does not eliminate static-electric forces between particles carrying charge and those conductive surfaces (even if the surface is 'grounded' so that it has no net charge). Some processes, like xerography, rely on being able to 'adjust' static-electric adhesion to be stronger than, or weaker than, van der Waals attraction between particles during different phases of the process [see box on xerography later]. In powder handling equipment, problem locations subject to charge build-up can sometimes be equipped with ion generators which flood the air at those locations with bipolar ions to neutralize the charge on the powder. Such charge cancellation processes are not evaluated in this paper.

In the most simplistic terms, two atoms 'touch' when the repulsion of the outer electron orbitals prevents the atoms from approaching closer. For atomic numbers greater than 10 this closest-approach distance is about 4Å, increasing slightly for higher atomic number atoms. When surface atoms in two approaching objects are separated by distances slightly greater than 'contact' or the closest-approach distance, a net attraction occurs due to induced dipole (and permanent dipole) interactions between the atoms. These dipole and other polar forces constitute surface-energy interactions which exist for all materials.

2. Surface-energy-related Attractive Forces

Van der Waals originally modified the ideal gas equation of state with two additional terms, one to account for the finite volume of the gas molecules and the other to account for an attractive force acting between molecules – which is responsible for liquid/vapor phase changes, among other macroscopic phenomena. For spherical atoms, the van der Waals forces can be thought of as arising from the instantaneous effective dipole of an orbiting electron (and its nucleus) inducing an effective instantaneous dipole in a nearby atom. The resulting dipole-dipole potential energy varies with, $1/d^6$, where d is the distance between the dipole centers of mass. A full quantum mechanical treatment of the energy of different configurations for two adjacent atoms [Feynman, 1939] confirmed that the classical electrodynamic equations were, for the most part, correctly describing these quantum-mechanical atom-atom interactions. Polar molecules *(i.e.* molecules with a permanent dipole moment) experience this interaction, and also interact with nearby molecules via permanent dipole/dipole and dipole/induced-dipole interactions. These interactions also have potential energies that vary as $1/d^6$, and are known as the Keesom and Debye energies, respectively. Collectively these three molecular-scale dipole interactions (London-dispersion [1930; 1937], Keesom [1921] and Debye [1920] energy) comprise what are currently known as van der Waals interactions (or forces) between molecules. All molecules (whether they are charged or not, have dipole moments or not, form Hydrogen bonds or not) are attracted to other nearby molecules by, at least the London-dispersion part of, the van der Waals interactions.

Surface energy (per unit area) is the work required to separate a unit area of two surfaces which are initially in intimate contact (on a molecular scale), and move them apart (doing work against the intermolecular forces of attraction) until the surfaces are infinitely far apart. Isrealachvili [1991] provides a thorough discussion of interaction energies between molecules and evaluation of the integrated effects of intermolecular interactions between all molecules in each of two spherical or planar objects separated a distance, s, apart (with particular emphasis on the case where the intermolecular potential varies with d^{-6}, where d is the distance between a pair of interacting molecules).

Planar Surfaces – Abreviating the discussion by

Isrealachvili [1991] consider a substance comprised of molecules which interact with an attractive pair potential of the form $\psi(dz) = -C_f/d^6$, where d is the distance between the molecules, and C_f is a constant. Next, consider a unit area of two planar surfaces, made of that material, which are a distance s apart. If we add all the contributions from all the $1/d^6$ pair interactions, and further integrate the resulting energy with distance, from the distance s to infinity, the result is the surface energy per unit area, as a function of the separation distance between the two planar faces, s,

$$w_p(s) = -\frac{\pi C_f \rho_a^2}{12 s^2} = -\frac{A}{12\pi s^2} \quad \text{(per unit area)} \quad (1)$$

where ρ_a is the volume density of atoms (molecules) in the material, and $A = \pi^2 C_f \rho_a^2$, is the Hamaker constant for the material [Hamaker, 1937].

Spheres – It can be shown [Derjaguin, 1934; Krupp, 1967; Isrealachvili, 1991] that the force, F_s, between two spheres of radii, R_1 and R_2, as a function of separation, s, is related to the surface energy per unit area (as a function of separation) for two planes (*i.e.*, Eqn 1) by,

$$F_s(s) = -2\pi R^* w_p(s), \quad (2)$$

where, $R^* = \dfrac{R_1 R_2}{R_1 + R_2}$.

If one sphere is very large, $R_2 >> R_1$ (approaching a sphere and a plane) Eqn 2 reduces to

$$F_{sp}(s) = -2\pi R w_p(s) \quad (3)$$

or, for two equal spheres,

$$F_{ss}(s) = -\pi R w_p(s). \quad (4)$$

Two important characteristics of van der Waals forces for spherical bodies can be deduced from these relationships (Eqns 1 – 4). First, we can substitute the expression of $w_p(s)$ from Eqn 1 into Eqn 2 to obtain the particle size and distance dependence of the attractive van der Waals force between two approaching spheres, or a sphere and a planar surface,

$$F_{vdW} = -\frac{A}{6 s^2} R^*. \quad (5)$$

Contact limit – Second, we can consider the limiting case when two bodies are in 'contact.' For two spheres in contact, where $s \approx s_o$ = molecular diameter $\approx 4\text{Å}$, the value of $w(s_o)$ can be associated with 2γ, where γ is the conventional energy per unit area of a surface. Thus, the force of adhesion (at contact) between two (undeformed) spheres, in terms of their surface energy is [Iseralachvili, 1991],

$$F_s(s_o) = F_c = -4\pi\gamma R^*; \quad (6)$$

which, for $R_2 >> R_1$, reduces to

$$F_{sp}(s_o) = -4\pi\gamma R \quad (7)$$

and, for two equal size spheres becomes,

$$F_{ss}(s_o) = -2\pi\gamma R. \quad (8)$$

This intimate relation between the planar surface energy per unit area and the cohesive force acting for sphere/plane contacts is one reason that surface energy is such a useful parameter characterizing cohesive forces of macroscopic bodies in contact. Real macroscopic bodies in contact seldom have intimate (*i.e.*, molecular-scale) planar surfaces touching. Instead, multiple surface asperities are in contact; however, each of these asperity-contacts can often be approximated as a sphere-sphere or a sphere-plane contact. The maximum difference between the attractive force for a sphere-sphere or for a sphere-plane contact is a factor of two [Krupp, 1967; Derjagiun, 1934]. Despite Isrealachvili's [1991] insistence that a sphere/plane contact can never respond like a plane/plane contact, when significant plastic deformation occurs in the contact region, the material within that region may closely resemble a plane/plane configuration wherein the cohesive force would be determined by the derivative of the energy-displacement relation, $\dfrac{-\partial w_p(s)}{\partial s}$, evaluated at contact, $s = s_o$, multiplied by the actual contact area (at the molecular level). For materials interacting with a van der Waals potential, varying with d^{-6}, this results in a force of cohesion at a planar contact (per unit area) of,

$$F_{cp} = -\frac{4\gamma}{s_o} \quad (9)$$

The significance of surface energy to cohesive/adhesive forces is apparent from Equations (6-9).
Refinements to these relations, taking into account elastic and/or plastic deformations in the contact region have been made by many researchers, but in all cases, the cohesive force at contact is directly proportional to the surface energy per unit area of the materials involved, whether the contact consists of an undistorted sphere touching a plane, a set of nearly spherical asperities in contact, or 'flattened' nearly

planar sub-regions in the contact area. Various theories differ in their interpretation of the effects of deformations in the contact region, yet all approaches show a direct relationship between the cohesive forces and the surface energy of the materials in contact. Knowledge of the surface energies of materials of interest, and estimates of the true area of contact are the key factors in being able to predict these surface-energy-related adhesive/cohesive forces acting on fine particles.

The Johnson, Kendall, Roberts (JKR) [1971] model for elastic cohesive contacts does not integrate the attractive forces over the two geometries of the contacting bodies, but instead, uses energy arguments and elastic deformation theory to account for the surface energy associated with separating elastically deformable spheres touching over a finite contact area. The model accounts for elastic deformation of the surface both in terms of the repulsive force 'flattening' the contact area (similar to a Hertzian elastic contact [Hertz, 1882]), and also a tensile region around the compressively loaded core region, increasing the size of the contact area over a purely compressive, Hertzian deformation. The JKR model predicts a pull-off force value of,

$$F_{c_{JKR}} = -3\pi\gamma R^*, \tag{10}$$

or a 25% lower value for the pull-off force over that predicted by Eqn (6) or the DMT [Derjaguin *et al.*, 1975] model. It is interesting to note that, while the JKR model is based on an analysis that includes elastic deformation of the spheres in the contact region (based on the Young's modulus and Poisson ratio of the material), the final expression for the pull-off force predicted by the JKR model is independent of the elastic constants used to obtain the force-displacement behavior.

Plastic deformation – By comparing the cohesive force between two spherical particles (Eqn 6, or 10) with the maximum load achievable for elastic spheres in contact before plastic deformation occurs, it can be shown that as particles get smaller they will eventually reach a size where the cohesive force will cause plastic deformation, even without any applied load. For example, for two equal-sized, non-cohesive, elastic spheres pressed together, the applied load at which plastic yielding begins, F_Y, varies with the square of the particle size [Johnson, 1985], *i.e.*,

$$F_Y = \frac{\pi^3 R^2 (1-\nu^2)^2}{6E^2}(1.6)^3 Y^3, \tag{11}$$

where E is Young's modulus, ν is the Poisson ratio for the material, and Y is the yield strength.

For cohesive particles in contact the pull-off force, F_c (e.g., Eqn 10) scales linearly with particle size, and it is generally accepted that at least a portion of the contact region will experience a repulsive force of the same order of magnitude as the pull-off force, F_c. For example, the force displacement relation for the JKR model is very similar in magnitude and shape to an elastic Hertzian force-displacement curve that has been shifted vertically by subtracting the cohesion force, F_c, from it (and also, perhaps, displacing it horizontally from the origin by an amount $a_s/2$, see **Fig. 1**).

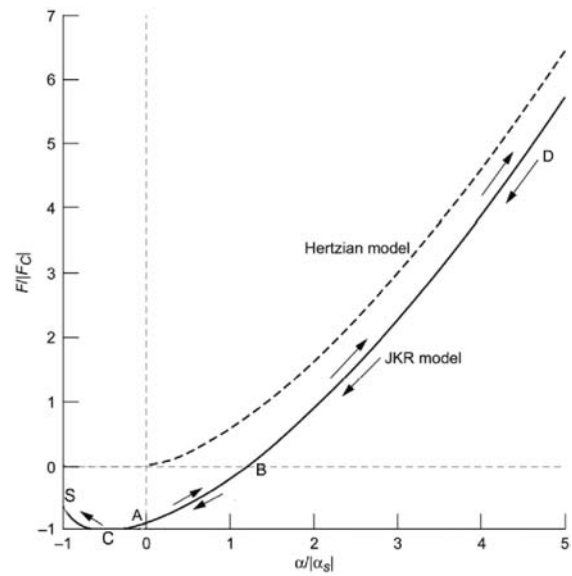

Fig. 1 Force-displacement curves for the cohesive JKR model and for a non-cohesive linear elastic Hertzian contact between two spheres. F_c is the cohesive pull-off force and a_s is the (outward) elastic displacement at final separation [Mei, 2000].

Setting F_c from Eqn 10 to F_y from Eqn 11, and further making the approximation (valid for many materials[Rabinovich, 1965]) that $Y \approx 0.003E$, and selecting $\nu = 0.3$ as a representative Poisson ratio, we obtain an estimate for the particle size, R_{cY}, below which plastic deformation would be expected for cohesive contacts, even with no applied loads,

$$R_{cY} \approx 1 \times 10^7 \frac{\gamma}{E}. \tag{12}$$

Table 1 shows the particle size (diameter) below which plastic deformation is likely due simply to the cohesional forces for two spheres in contact, without any external loads, for various values of Young's modulus, E, and surface energy, γ (assuming $\nu = 0.3$, and $Y \approx 0.003E$).

Table 1 Particle diameter below which plastic deformations occur at contacts

$E\downarrow$ and $\gamma\rightarrow$	20 mJ/m^2	200 mJ/m^2	2000 mJ/m^2
1GPa	400μm	4mm	40mm
10GPa	40μm	400μm	4mm
100GPa	4μm	40μm	400μm

When the effects of plastic deformation, such as the broadening of the stress distribution and the widening of the contact area, are taken into account, it is observed that the plastically deformed contact region is 'flattened,' but is not truly flat. Upon unloading, the region often behaves like an elastic sphere with a larger radius. As the effective radius of the 'flattened' area increases, the effective pull-off force increases. By the time significant plastic deformation is occurring in the contact region the effective radius of the contact spot during unloading might be increased by as much as a factor of two. One approximation of the adhesive-elastic unloading from such a contact is simply a JKR model with a factor of two greater radius of curvature, $R_p \rightarrow 2R$ [Thornton & Ning, 1998]. The net effect is to increase the pull-off force, F_c by up to a factor of two,

$$F_{c-plastic} \approx -6\pi\gamma R^*. \tag{13}$$

More complex expressions describing the transition from elastic to plastic behavior have also been developed (e.g., Margus & Pollock [1974]) however, the net attraction force is within the bounds already discussed. An additional case, for extremely compliant surfaces, where total particle engulfment is possible, is described by Rimai, *et al* [1994; 1995]; however such soft surfaces are not often used in powder handling equipment.

Measurements of surface forces and energy – A variety of methods exist to measure surface energy of solid surfaces and powdered materials utilizing various 'probe' liquids or gases. Typical surface energies range from 20 to 2000mJ/m^2, and are often in the range of 40 to 100mJ/m^2. Evaluation of Eqn 7 with surface energies in this range, predicts a pull-off force of a few micro-Newtons for a 10μm diameter particle. AFM measurements on 8μm diameter spherical particles (of glass, polystyrene, and tin) contacting atomically flat surfaces, however, resulted in lift-off forces which were typically a factor of 50 less than 'predicted' values [Schaefer et al, 1995]. A detailed AFM mapping of the surface asperities and reinterpretation of the contacts as occurring between multiple asperities and the flat substrate, brought the theory and experiments to within a factor of 3 of each other (with the predicted pull-off force still greater than the measured values, but close enough that possible surface contamination could explain most remaining differences). Similarly, centrifuge measurements of the average adhesion forces on uncharged irregularly shaped toner particles, of nominally 10μm diameter, are as high as 50nN [Hays, 1994] (but nearly two orders of magnitude smaller than would be the case for perfectly smooth spheres of the same size). Also, many irregularly shaped pharmaceutical powder particles, ranging in size from 1μm to 200μm, have been tested on 'functionalized' AFM tips by numerous researchers. Generally the (statistical average of the) forces measured, scale directly with the particle size – as expected from JKR (or Derjaguin) theory; and they also, usually scale directly with surface energy (when it has been separately measured). Typical pull-off forces range from 2 to 40nN for micron-scale particles and from 10's of nN up to ~500nN for 100μm scale particles under low humidity [Nagai, 2005]. These values are considerably lower than values predicted for smooth spherical particles (e.g. Eqn 7 or 8). An evaluation of the distance dependence of van der Waals forces for particles near surfaces (e.g. Eqn 5) and a comparison with the range-of-effect of other ostensibly inverse square forces (such as electrostatic forces) can elucidate why the surface energy related forces are so sensitive to surface roughness and estimates of the area of contact, yet, electrostatic forces are relatively insensitive to surface roughness in the contact region. This range-of-effect behavior is discussed in more detail after the section below describing image-charge forces acting on particles. Walton [2007] provides a brief review of various methods utilized to measure surface energies of solids and particulate materials.

3. Image-charge Forces

When a charged particle is near a conducting surface, the charge on the particle induces a redistribution of charge in the conductor. Because the electric field at the surface of a conductor is always perpendicular to that surface (or there would be currents flowing on the surface), it follows that the potential on that surface is always a constant. That boundary condition can be satisfied by considering the field produced by an 'image' charge of opposite sign, located the same distance 'inside' the conductor that the center of charge is 'above' the surface. By uniqueness, the combined electric field from the pri-

mary charge and the image charge correctly describes the electric field in the vicinity of the charge near a conducting surface. The electrostatic Coulomb force acting on a point charge, Q, due to its image 'inside' the conductor is

$$F_I = -\frac{QQ'}{4\pi\varepsilon_0 D^2}, \tag{14}$$

where Q' is the image charge (equal in magnitude to Q), and D is the distance between the charge and its image $D = 2h$, where h is the height of the charge above the surface. For a finite-size particle, of diameter D_p, carrying a charge uniformly distributed on its surface, a similar relation holds, and $D \approx (D_p+s)$, where s is the 'gap' spacing between the sphere and the conducting surface. To correctly account for finite sized particles comprised of real dielectric materials the dipole and higher moment distributions induced by the image charge also need to be taken into account. The orientation of the dipoles are such as to increase the attraction due to the monopole terms, so that Eqn (14) represents a lower bound on the image charge force on a spherical particle (near a conducting surface) with a uniformly distributed charge Q on the particle's surface.

Approximating an irregularly shaped dielectric particle as spherical, and further approximating the additional contribution from polarization with a correction factor, β, the electrostatic image force on the particle near a planar, conductive substrate is given approximately by,

$$F_I \approx -\beta\frac{Q^2}{4\pi\varepsilon_0(D_p+s)^2} \tag{15}$$

where Q is the particle charge, D_p is the average diameter, ε_o is the permittivity of free space and β is a correction factor which depends on the polarization of the dielectric particle. (For a dielectric constant of $\kappa = 4$, $\beta = 1.9$ [Hays, 1988]). For a typical toner particle used in xerography with a charge-to-mass ratio of 15 mC/kg and an average toner diameter of $10\mu m$, the particle charge, Q is $8fC$, and the electrostatic image charge as calculated from Eqn (15) with $s << D_p$ is ~$10nN$.

Particles can attain charge from a variety of causes; however, the most common source of charge build-up in powder handling is triboelectric charge transfer. Tribocharging is likely to result in non-uniform distributions of charge over particle surfaces. The non-uniformity in charge distribution on particles can play a significant role in the adhesive effects of the charge.

Fig. 2 shows measured average toner adhesion forces obtained from centrifuge measurements compared to the image force model calculations (*i.e.*, Eqn. 15 with $s \approx 0$) as a function of the average toner charge-to-diameter ratio [Hays, 1994]. The measured values exceed the predictions of the uniform surface charge model by factors of from 5 to 50. The dependence of the measured adhesion on charge ratio eliminates van der Waals adhesion forces as an explanation for the difference, since surface adhesion forces would be independent of charge. (Note that typical toner particles are usually 'dusted' with a small quantity of ultra-fine fumed-silica to reduce the van der Waals forces to something on the order of ~$10nN$, see box on xerography). Hays [1994] proposed that the total charged area A_t on a tribo-electrically charged toner particle represents a small part of the total toner particle's surface area. Based on Hays' model, the total charge would be $Q = \sigma A_t$, where σ is the surface charge density (in the charged regions). A small fraction, like 20%, of the charged surface area, A_c, might be in close proximity to the conducting surface. If the extent of the charged areas in close proximity, A_c, is much larger than the average distance between the charged surface and the conducting substrate, the magnitude of the electrostatic forces of adhesion can be expressed as, $F_E = -\frac{\sigma^2 A_c}{2\varepsilon_0}$, and the total adhesion can be written as,

$$F_A = -\frac{\sigma^2 A_c}{2\varepsilon_0} - WA_c, \tag{16}$$

where WA_c represents a non-electrostatic (*i.e.*, surface-energy based) adhesion contribution. Literature estimates indicate contact charging can produce surface charge densities ranging from 0.5 to $5mC/m^2$ depending on the materials involved [Horn and Smith, 1992]. For $\sigma = 1mC/m^2$ and $Q = 8fC$, the electrostatic contribution to the adhesion force is ~$100nN$, which is comparable with measured values for toner particles [Hays, 1995].

Gady [1996] performed a series of AFM measurements on $3\mu m$ and $6\mu m$ polystyrene spheres (attached to an AFM cantilever and) brought toward an atomically flat, highly oriented pyrolytic graphite (HOPG) substrate. Polystyrene and HOPG lie at opposite ends of the tribocharging sequence (*i.e.*, they have large differences in their respective work functions) and thus can produce significant tribo-charging upon contact and separation. Gady used the change in frequency of a small driven oscillation of the cantilever to precisely determine the force and force gradient as functions of separation from the sub-

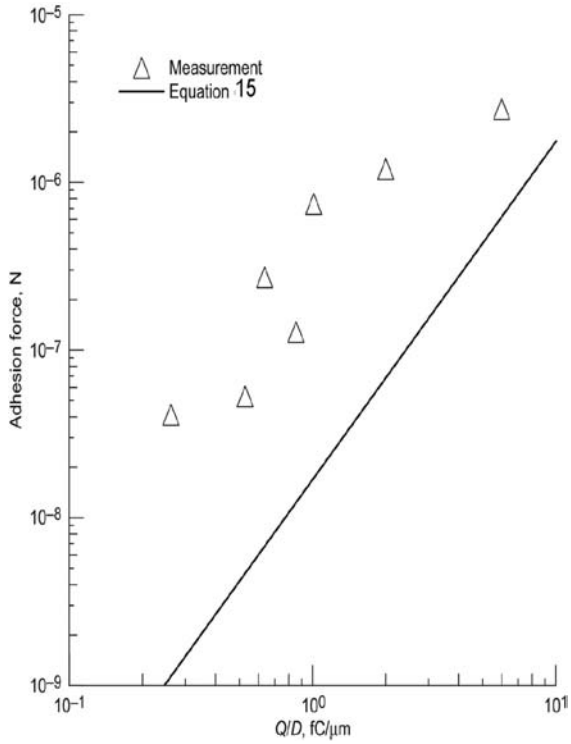

Fig. 2 Toner adhesion forces obtained from centrifuge measurements compared with image force model calculations (Eqn. 15 with $s \approx 0$, which assumes charge is distributed uniformly over the particle's surface) as a function of the average toner charge-to-diameter ratio [Hays, 1994].

strate. By first contacting the substrate, to establish a precise position for 'contact', and then separating the sphere from the substrate and operating in a non-contact mode, Gady was able to map the force-separation relation (until the snap-to-contact point when the sphere was a few nano-meters above the surface). Since local charge patches in the region of contact produced high local electric fields ($\sim 2.5 \times 10^8$ *V/m*), these measurements were conducted under a modest vacuum (10^{-2} Torr) in order to avoid discharge via breakdown in air. **Fig. 3** shows a representative force displacement curve for a $3\mu m$ polystyrene sphere. Also shown are theoretical curves for van der Waals force and an electrostatic force based on an assumed charge patch located within a sphere (inside the particle) collocated with the contact spot and having a radius equal to the JKR contact spot radius. The solid line on the **Fig. 3** is the sum of the two theoretical curves. The cross-over point where the van der Waals exceeded the charged-patch electrostatic force (for these highly-charged contacts) varied from 3*nm* to 10*nm* depending on the charge on the sphere. At separations closer than the crossover point van der Waals forces dominated the attractive force measured. (Not shown is a curve that would be appropriate for a charge uniformly distributed over the surface of the polystyrene sphere. Such a force-displacement curve would be lower in magnitude and much lower slope than the patch-charge curve at close separations).

Gady's small charged sphere analysis simplifies the mathematics somewhat over having the charge located only on a patch of the particle surface material; however, it still captures most of the physics of having the tribo-electric charge located near the contact region. Gady's approach is equivalent to modifying Eqn 15 to represent the image charge force due to a local charge patch of diameter $D_Q = 2a$, where a is the JKR contact spot radius,

$$F_{I_L} \approx -\beta \frac{Q_L^2}{4\pi\varepsilon_0 (D_Q + s)^2}. \tag{17}$$

A more complex mechanism than localized charge-patches, involving a non-uniform distribution of effective electron work-function values over the surface of particles, has also been proposed as an explanation of the high electrostatic attraction for small charged particles [Pollock, et al, 1994]; however, the simpler localized tribo-charged patches as described by Hays [1994] and/or Gady [1996; and Gady *et al*, 1996] appear to adequately describe the observed phenomena. In Gady's experiments with spherical particles near a smooth substrate, the van der Waals force did not dominate over image-charge forces until the gap spacing was on the order of 10*nm*. Most irregularly shaped particles produced through comminution would have surface roughness at least as great as 10's of nanometers, lowering the effective attraction at contact by an order of magnitude or more.

4. Distance-dependence and Range-of-effect of Fine-particle Adhesive Forces

Range of effect – The electric field in the vicinity of a large charged surface (like the nearly uniformly charged lunar surface) decreases very slowly with distance away from the surface. The static-electric force on a charged particle in such a slowly varying electric field, likewise, varies slowly with distance. Because of their relatively long range nature, electrostatic forces have the potential to contribute both as long-range forces affecting *motion* of fine particles (especially for suspended particles) and as short-range forces affecting their *adhesion/cohesion*, depending on the net charge on a particle and on the surface charge-density near a contact point. While van der Waals forces, electrostatic forces between

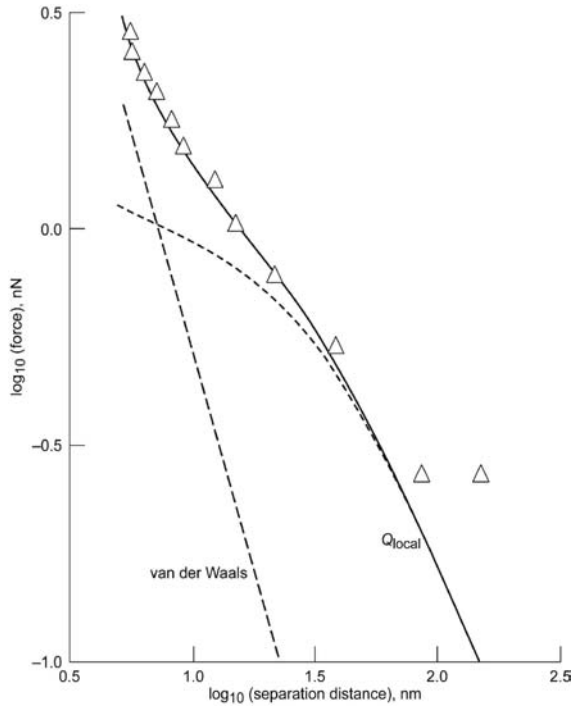

Fig. 3 AFM-measured force-displacement for a triboelectrically charged 3μm polystyrene sphere near an atomically flat HOPG substrate (symbols), van der Waals force *(i.e.*, Eqn. 5) (dashes), and a local charged-patch (of a JKR-contact-spot size, *i.e.*, Eqn 17) with Q_L adjusted to best fit the data (dotted line). Solid line is sum of van der Waals and charged-patch curves [Gady et al, 1997].

charges, and electrostatic image-forces, all vary as the inverse square of distance; the effective *distance* at closest approach (where the force has its maximum value) differs in each case. As described by Eqn 5, the net van der Waals force for a single spherical/planar contact (asperity or particle) depends on the distance between the centers of the surface atoms in the two bodies at their point of closest approach. This inverse square relation is not a fundamental property of the dipole forces which comprise the van der Waals interaction. Those forces all decay with the inverse seventh power of the distance on a molecular level. The inverse second power comes from the integrated effect of all (relatively near) atoms in a sphere and in the nearby plane. It should also be noted that at distances greater than approximately 10*nm*, retardation effects, of induced dipoles on the molecular level, begin to reduce the effective van der Waals interaction below that predicted by Eqn 5. Such effects are usually modeled as reductions in the Hamaker constant with distance beyond 10*nm* [Isrealachvili, 1991]. Thus, for a variety of reasons, surface-energy related adhesion forces are very short range and primarily affect fine particles when they are in contact with each other or touching surfaces. The electrostatic force on the other hand varies as the inverse second power of the distance between the two apparent centers of charge. If we consider the distance over which a force decreases by a fixed factor, say two orders of magnitude, below its maximum value at 'closest approach,' as one measure of the range-of-effect of that force, then we can see significant differences between the *effective ranges* of these three inverse-distance-squared forces (*i.e.*, Eqns 5b, 15b, and 17b),

$$F_{vdW} = \frac{K_{vdW}}{s^2} \qquad \text{van der Waals interaction} \qquad (5b)$$

$$F_I \approx \frac{K_I}{(D_p + s)^2} \qquad \text{Image charge force – uniform charge on particle of diameter, } D_p \qquad (15b)$$

$$F_{l_L} \approx \frac{K_{L_I}}{(D_Q + s)^2} \qquad \text{Image charge force – local charge patch, diameter} \approx D_Q \qquad (17b)$$

Xerography

(A technology utilizing tribo-charging and electrostatic transfer of fine particles)

Researchers and technologists developing and improving electrophotographic processes (Xerography) have been successfully charging, transporting, removing and precisely depositing 10 micron-scale toner particles onto and off of various surfaces for nearly 50 years. Since its introduction (late 1950's) much of the development in xerographic technology has been by cut-and-try engineering methods. During the last two decades, our understanding of the underlying principles and forces involved in xerography have advanced dramatically, especially with the advent of various surface-force and scanning-probe measurement methods. Nonetheless, a cursory survey of current literature on particle adhesion, shows that, even today, several aspects of the process remain incompletely understood. [The following qualitative description, most closely fits the dry-powder xerographic technology of about a decade ago, when it was dominated by black-and-white dry-powder methods, but it still provides insight on methods that have been utilized to 'control' electrostatic- and tribo-charging of fine particles].

Xerography (continued)

The mechanics of the xerographic process require both electrostatic adhesion/cohesion and interparticle surface-energy-related forces to dominate at different stages. The average surface cohesive forces acting among the toner particles are usually 'adjusted' to a fixed (relatively low) value by blending the toner particles with nano-scale (~20nm − 40nm) fumed-silica fines with a weight −fraction of fines in the range of 0.01% to 1%. These fines, deposited on the larger-particle surfaces, act as *props* to keep most of the potential surface area at contacts far enough apart that the short-range van der Waals surface forces are greatly reduced. The relatively small contact area of the few propping fines, and the remaining contacting asperities on the particles, provide an appropriate level of cohesion for the process to work.
In xerography the toner particles are triboelectrically charged by mixing with larger carrier beads. The charge on the toner particles enables the electrostatic transfer of these particles between surfaces, allowing the development of an electrostatic latent image and subsequent transfer of the developed image to paper. Because of the requirement for toner transfer, the cohesion and adhesion properties of toner particles are of considerable importance in optimizing the electrophotographic process [Hays, 1995; Pai and Springett, 1993].
In xerography tribocharging is controlled through selection of the material, for the carrier beads (with an appropriate value for its work-function) and toner particles, and by the intensity and duration of 'mixing'. The surface energy forces are controlled by adjusting the mass fraction of ultra-fine fumed silica blended with the toner; and, the electro-static force is controlled by the electric fields/potentials applied externally. Many of these quantities will be beyond the control of lunar explorers and in-situ resource utilization designers dealing with fine particles occurring on the moon's surface (and they may not be controllable in terrestrial powder processing operations).

where the K's and D's depend on material, size and/or charge but do not change with distance, s.

At 'contact' the distance between surface molecules centers, s_o, is approximately 4$\AA$ (or ~0.4nm), and $D_b >> D_Q >> s_o$, so that the closest approach values of the denominators in these relations are usually much larger for electrostatic forces than the molecular-scales of van der Waals forces.

The van der Waals force which varies as the inverse second power of the *gap spacing* (e.g., Eqn 5b), is a very short-range force compared to typical particle dimensions − falling by two orders of magnitude by the time the surfaces are 40$\AA$ (~4nm) apart, and by four orders of magnitude by the time they are 40nm apart. In comparison, an image-charge force for a charged particle near a conducting surface, Eqn 15b, would decrease two orders of magnitude over a separation distance from touching (e.g. 1-diameter) to ten *particle* diameters (a distance of 10μm for a 1μm particle, or 100μm for a 10μm particle). The image-force from a small patch of concentrated charge on a particle's surface (Eqn 17b), say 100nm across, would also decrease more slowly than the van der Waals force (Eqn 5b). On a 10μm particle, a 100nm diameter patch-charge image-force would decreasing two orders of magnitude going from contact with a conductor to a separation distance of approximately 1μm, according to Eqn 17b. This is 250 times the distance over which van der Waals force would decrease by two orders of magnitude. Thus it can be inferred that the image-force for a uniformly charged particle is, in effect, longer-range than the local charged-patch force, which is, in effect, longer-range than the van der Waals force.

Because their values change less rapidly with distance (near contact), the static-charge forces are less affected by surface asperities and roughness than are van der Waals forces. Thus, for small irregular particles coated with a light dusting of nano-scale fines (as is the case for xerographic toner particles) it is possible, with sufficient local charge deposition, for localized charge-patch forces to dominate over van der Waals surface forces even when the particles are 'contacting' the surface. Such may also be the case for small tribocharged lunar dust particles, or other fine irregular particles.

5. Effects of Particle Size on Fine-particle Adhesive Forces

One of the aims of this review is to determine under what conditions various forces are likely to domi-

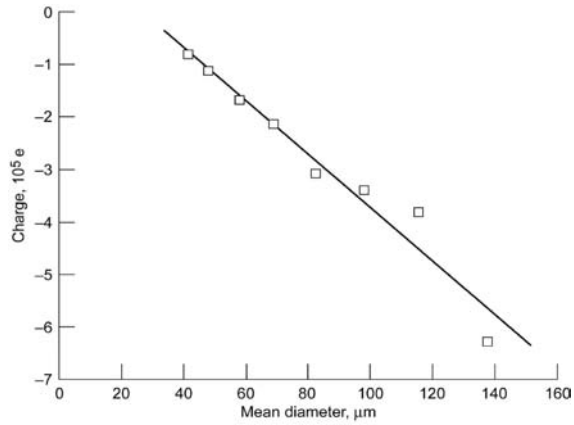

Fig. 4 The charge on JSC-Mars-1 from a contact with a Co surface for different dust sizes [Sternovsky *et al*, 2002].

nate in the adhesion of particles to surfaces. Because of the way surface forces scale relative to body forces and drag forces, surface phenomena are usually expected to dominate at small particle sizes. Gravity and inertial forces (*e.g.*, response to vibration, shaking or acceleration) scale with the mass of an object, $M = \rho V = \rho(4/3)\,\pi R^3$, where ρ is density (*e.g.*, kg/m^3), V is volume (*e.g.*, m^3) and R is the 'radius' of the object (assuming a spherical shape). Thus, as particles decrease in size the force of gravity, and that due to accelerations, would decrease with the cube of the particle size. The aerodynamic drag at high Reynolds numbers scales with the cross-sectional area of an object in the flow. As particle size decreases high-Reynolds-number drag forces decrease with the square of the particle size. Likewise, the surface area of a particle decreases with the square of its diameter. Thus, we might expect that most surface related phenomena will scale with the square of particle size (like the surface area). In fact, many phenomena, including some surface related ones, decrease more slowly with particle size than the square. Several important phenomena scale nearly linearly with particle size. As particle size decreases, phenomena which scale linearly with size will eventually dominate over phenomena that scale with higher powers of the size (like gravity, inertial forces, or high-Reynolds-number drag forces). Among phenomena that scale linearly with size, other controlling parameters need to be examined in order to determine which will have a greater influence on particle motion or behavior.

As previously described, the integrated effects of van der Waals interactions acting on a spherical particle near a surface (e.g., Eqn 5) depends linearly on the radius of curvature in the contact region (e.g., the van der Waals force varies linearly with particle size).

It is also well known that the electrical capacitance of an isolated conducting sphere depends linearly on the size of the sphere [Corson & Lorrain, 1962],

$$C = 4\pi\varepsilon_o R_p. \tag{18}$$

The charge carried by a particle with a uniform surface potential, Φ_s, is proportional to its capacitance,

$$Q = C\Phi_s = 4\pi\varepsilon_o \Phi_s R_p, \tag{19}$$

a quantity which varies linearly with particle size. In a uniform electric field, **E**, the force on a charged particle, also, would vary linearly with particle size,

$$\mathbf{F_E} = Q\mathbf{E} = 4\pi\varepsilon_o \Phi_s \mathbf{E} R_p. \tag{20}$$

While the formula for capacitance (Eqn 18) is strictly valid only for conducting spheres, experimental evidence indicates that triboelectric charging of non-conducting particles, also, varies nearly linearly with particle size.

Fig. 4 shows the dependence of tribocharge with particle size for simulant JSC-1-Mars-1 particles, each experiencing the same type and duration of repeated contact with a Co surface [from Sternovsky *et al*, 2002].

It should be noted that, the static image-charge force, F_I, acting on a charged particle depends on the square of the charge on the particle, and if non-conducting particles carried uniformly distributed surface charges varying with size according to Eqn 19 and they were in contact with a conducting surface, they would experience an attractive image-charge force of,

$$F_I \approx \pi\varepsilon_o \Phi_s^{\,2} \approx 0.05\ \Phi_s^{\,2}\ (nN/V^2), \tag{21}$$

independent of particle size! For particle sets comprised of particles with net charges proportional to their size, we would expect that below some threshold size, image-charge adhesion forces would dominate over surface-energy related forces.

Under certain circumstances, sets of particles are more likely to acquire charges that vary according to their effective cross-sections, and thus would be expected to have net charges that vary with the square of the particle size. For example, charging of micron-scale conductive aerosol water droplets via capture of like-charged ultra-fine particles in the upper reaches of thunderstorms results in a maximum charge per droplet that varies approximately with the square of the droplet size [Pruppacher & Klett, 1997, as cited in Tinsley et al, 1999]. For particle sets with charge distributions that scale with the square of particle size, the effective image-charge forces at contact would decrease in direct proportion with the particle

size, and fine-particle adhesion would be dominated by surface-energy interactions.

Discussion

From the works of London, Hamaker, Feynman, Lifshitz, Keesom, Debye and others we have a reasonably good understanding of the molecular-scale sources of van der Waals forces; however, the integrated macroscopic effects of van der Waals forces as described above are only straightforward to calculate for idealized configurations. For most real contacts between macroscopic objects, the adhesive forces can differ substantially from what would appear to be a straightforward integration of a known intermolecular potential over all nearby molecular centers. It is the relatively short-range nature of van der Waals forces (from a macroscopic perspective) which give rise to much of the 'uncertainty' in calculating their effects for real macroscopic contacts. As pointed out by Isrealachvili [1991] one source of uncertainty in predicting adhesion forces from models of van der Waals interactions is uncertainty associated with the effective surface energy, since even monolayers of gas molecules adsorbed on a surface can affect the value of the adhesive force at contact. Two other factors which contribute significant uncertainty to making quantitative predictions of adhesion forces are *surface morphology* (or roughness), and *deformation* (elastic and plastic) in the contact region. Measurements of pull-off forces for small particles, can be substantially less than the values predicted a *prori* from known surface energies or Hamaker constants for the materials involved, with the over prediction by the theory increasing as the particle size decreases. Large soft spheres, on the other hand, adhere in almost exact agreement with the Johnson, Kendall, Roberts (JKR) theory [1971]. JKR theory accounts for elastic deformation in the contact region, but is still within 30% of the Derjagian approximation for undeformed spheres, e.g. Eqn (6), at contact. Surface roughness (e.g. detailed surface morphology) has been identified as one major contributor to the discrepancy between measured pull off forces for 'real' particles and theoretical predictions for smooth surfaces [Rabinovich, et al, 2000 and 2002; Rimai & Quesnel, 2001; Mizes, 1994; Schaefer et al, 1995]. Likewise as the particle size (or the radius of curvature in the contact region) decreases, it is possible for plastic deformations to occur at the contact, even with no external loads; however, plastic deformation are usually expected to cause less than a factor of two increase in effective adhesion forces (unless external loads are also applied to the contacting bodies).

Because of the short-range nature of adhesive surface forces, it can be said with some certainty that adhesive surface forces are likely to be a major concern *only* when attempting to remove particles from surfaces. Under most circumstances, surface forces will have *only a minimal contribution* as to whether or not particles make contact with surfaces. [This is contrary to the potential effects of surface forces on particles in a third media, like in aqueous suspensions, where net surface forces can have a strong influence on whether 'contact' occurs]. Static electric forces, and in particular, image-forces, can be a significant factor in adhesion. These forces have a much longer effective-range than surface energy interactions. Thus they can have a significant effect on both the *motion* and on the *adhesion* of fine particles on surfaces.

Rough estimates of distance ranges over which various force are likely to dominate (for 10-*micron*-scale particles under dry conditions) might be summarized as follows, where, s is the distance between a particle and a (conducting) surface:

- $s > 0.1$ micron, electrostatic forces due to the *net charge* on particles may dominate
- $100nm > s > 10nm$, electrostatic forces due to localized *charge patches* on particle surfaces may have a significant effect
- $s < 10nm$, van der Waals (surface energy related) forces may dominate (if surfaces are smooth enough and/or surface energies high enough).

Very rough, irregular particles or particles with a dusting of nano-scale fines may have very low effective van der Waals adhesion forces. For such cases, the electrostatic and image forces can exceed surface energy forces for particles considerably larger than 10 microns (and/or with lower charge densities than are typical in xerographic processes).

Acknowledgments

This work was supported by NASA under contract NNC06VC87P. The project manager for this work was Dr. Allen Wilkinson, Glenn Research Center. Dr. Wilkinson's encouragement and patience and NASA's support are gratefully acknowledged.

References

Corson, D.R., and Lorrain, P. (1962): "Introduction to Electromagnetic Fields and Waves", W.H. Freeman & Co. San Francisco and London.

Debye, P. (1920) : Phys Z., 21, p.178.

Derjaguin, B.V. (1934) : Kolloid Zeits, 69, pp.155-164.

Derjaguin, B.V, Muller, V.M. and Toporov, Y.P. (1975) : J. Colloid Interface Sci, 53, pp.314-326.

Feynman, R.P. (1939): Forces in Molecules, Phys. Rev. 56, pp.340 – 343.

Gady, Barrett, L. (1996): Measurement of Interaction Forces Between Micrometer-Sized Particles and Flat Surfaces Using an Atomic Force Microscope, PhD Thesis, Purdue University.

Gady, B, Reifenberger, R., Rimai, D.S. and DeMejo, L.P. (1997): Langmuir 13, pp.2533-2537.

Gady, B, Schleef, D., Reifenberger, R., DeMejo, L.P. and Rimai, D.S. (1996): Phys Rev B, 53, pp.8065-8070.

Hamaker, H.C. (1937): Physica 4, pp.1058-1072.

Hays, D.A. (1988) : in "Particles on Surfaces 1", Detection, Adhesion and Removal, K.L. Mittal (Ed.) pp.351-360, Plenum Press, NY.

Hays, D.A. (1994): Toner Adhesion, "Advances in Particle Adhesion", pp. 41-48, D.S. Rimai, and L.H. Sharpe (Eds).

Hays, D.A. (1995): Adhesion of Charged Particles, "Fundamentals of Adhesion and Interfaces", pp. 61-71 D.S. Rimai, L.P. DeMejo, and K.L.Mittal (Eds), VSP Utrecht, Netherlands.

Hertz, H. (1882): Über die Berührung fester elastische Körper (On the contact of elastic solids), J. reine und angewandte Mathematik, 92, pp.156-171. (for English translation see Miscellaneous Papers by H .Hertz, (Eds) Jones and Schott, London, Macmillan, 1896)

Horn, R.G., and D.T. Smith (1992): Science 256, pp.362-364.

Keesom, W.H. (1921): Phys Z., 22, p.643.

Krupp, H. (1967): Particle Adhesion, Theory and Experiment, Adv. Colloid Interface Sci., 1, pp.111-239.

Isrealachvili, J. (1991): "Intermolecular and Surface Force", 2nd Ed. Academic Press (Elsevier).

Johnson, K.L., Kendall, K. and Roberts, A.D. (1971): Surface energy and the contact of elastic solids, Proceedings, Royal Society, A324, pp.301-313.

Johnson, K.L. (1985): "Contact Mechanics", Cambridge Univ. Press, London.

Lian, G., Thornton, C., Adams, M.J. (1993): A theoretical study of the liquid bridge forces between two rigid spherical bodies, J. Coll. Int. Sc., 161, pp.138-147.

London, F. (1930): Z. Phys. Chem, B11, pp.222-251.

London, F. (1937): Trans. Faraday Soc, 33, pp.8-26.

Maugis, D., and H.M. Pollock, (1984): Acta Metall. 32, pp.1323-1334.

Mei, R., Shang, V, Walton, O.R. and Klausner, J.F. (2000): Concentration non-uniformity in simple shear flow of cohesive powders, Powder Technol., 112(1-2), pp.102-110.

Mizes, H.A. (1994): Surface Roughness and Particle Adhesion, "Advances in Particle Adhesion", D.S. Rimai & L.H. Sharpe (eds) Gordon & Breach Pub. pp.155-165.

Nagai, S.S.H. (2005): Multi-Scale Analysis and Simulation of Powder Blending in Pharmaceutical Manufacturing, Thesis, Massachusetts Institute of Technology, Chemical Engineering.

Pai, D.M., and Springett, B.E. (1993): Rev. Modern Phys. 65 (1), pp.163-211.

Pollock, H.M., Burnham, N.A. and Colton R.J. (1994): Attractive Forces Between Micron-Sized Particles: A Patch Charge model, D. S. Rimai and L.H. Sharpe (Eds.) , "Advances in Particle Adhesion", pp.71-86, Gordon & Breach Pubs.

Pruppacher, H.R., and Klett, J.D. (1997): "Microphysics of Clouds and Precipitation", 2nd ed. Kluwer, p.954.

Rabinowicz, E. (1965): "Friction and Wear of Materials", John Wiley and Sons, NY

Rabinovich, Y. J., Adler, J., Ata, A., Singh, R. and Moudgil, B. (2000): Colloid Interface Sci. 232, pp.10-16, and pp.17-24.

Rabinovich, Y., Adler, J., Esayanur, M., Ata, A., Singh, R. and Moudgil, B. (2002): Adv. Colloid Interface Sci. 96, pp.213-230.

Rimai, D.S., Demejo, L.P. and Bowen, R.C. (1994): The Adhesion of Particles to Polymer Coated Substrates, "Advances in Particle Adhesion", p139-154, D.S. Rimai and L.H. Sharp (eds) Gordon and Breach Pub, Amsterdam,.

Rimai, D.S., Demejo, L.P. and Bowen, R.C. (1995): Mechanics of Particle Adhesion, "Fundamentals of Adhesion and Interfaces", pp1-23, D.S. Rimai, L.P. DeMejo and K.L. Mittal (eds) VSP.

Rimai, D.S., and Quesnel, D.J. (2001): "Fundamentals of Particle Adhesion", Global Press.

Salisbury, J.W., Glaser, P.E., Stein, B.A. and Vonnegut, B. (1964): Adhesive Behavior of Silicate Powders in Ultrahigh Vacuum, J. Geophys. Res. 69, pp.235-242.

Schaefer, D.M., Carpender, M ., Gady, B., Reifenberger, R., Demejo, L.P. and Rimai, D.S. (1995): Surface roughness and its influence on particle adhesion using atomic force techniques, "Fundamentals of Adhesion and Interfaces", pp. 35-48.

Sternovsky, ?, Zoltán, ?, Robertson, S., Sickafoose, A., Colwell, J. and Horányi, M. (2002): Charging of lunar and Martian Dust Simulants, Journal of Geophysical Research, 107, No. E11, 5105, doi:10.1029/2002JE001897.

Thornton, C. and Ning, Z. (1998): A theoretical model for the stick/bounce behaviour of adhesive elastic-plastic spheres, Powder Technology, 99, pp.154-162.

Tinsley, B.A., Rohrbaugh, R.P., Hei, M. and Beard, K.V. (2000): Effects of image Charges on the Scavenging of Aerosol Particles by Cloud Droplets and on Droplet Charging and Possible Ice Nucleation Processes, J. Atmospheric Sci. 57, pp.2118-2134.

Walton, O.R. (2007): Adhesion of Lunar Dust, NASA/CR-2007-214685, NASA report available as pdf file at: http://gltrs.grc.nasa.gov/reports/2007/CR-2007-214685.pdf.

Xue, X. and Polycarpou, A.A. (2007): An improved meniscus surface model for contacting rough surfaces, Journal of Colloid and Interface Science、311-1, pp.203-211.

Nomenclature

A	Hamaker constant	[J]
A_t	Total surface area (of a charged particle)	[m^2]
A_c	Area of the charged portion of a particle's surface	[m^2]
Å	Angstrom − length unit = 10^{-10} m, or 0.1nm	
a	Relative approach distance (after initial contact) between two spheres, also amount of overlap that would have occurred without surface deformation)	[m]
a_s	Surface displacement (negative) in tension at separation (JKR model)	[m]
C	Capacitance	[C/V]
C_f	Material dependant constant (for interatomic force relation)	[$m^7kg^{-1}s^{-2}$]
d	Distance between centers of atoms	[m]
D	Distance between charges	[m]
D_p	Diameter of a (charged) particle	[m]
D_Q	Diameter of a local charge patch	{m]
ε_0	Permittivity of free space	[8.8542×10^{-12} C^2 N^{-1} m^{-2}]
E	Youngs modulus	[GPa]
E	Electric field (in Eqn 20 only)	[V/m]
F	Force	[N]
F_c	Cohesive (attractive) pull-off force	[N]
F_{cJKR}	Cohesive pull-off force JKR model	[N]
F_{cp}	Cohesive force per unit area for two planes in contact	[N/m^2]
$F_{c\text{-}plastic}$	Approximate cohesive force for plastically deformed spheres in contact	[N]
$\mathbf{F_E}$	Electrostatic portion of the force of adhesion	[N]
F_T	Total force of adhesion including both electrostatic and surface-energy terms	[N]
F_I	Electrostatic image-charge force acting on a charge near a conducting surface	[N]
F_{IL}	Electrostatic image-charge force due to a local charge patch near a conducting surface	[N]
F_{vdW}	van der Waals cohesive/adhesive force	[N]
F_s	Cohesive (attractive) force acting between (undeformed) contacting spheres	[N]
F_{ss}	Cohesive force acting between two equal size spheres	[N]
F_{sp}	Cohesive force acting between a sphere and a plane	[N]
F_Y	Applied load at which plastic yielding begins	[N]
$\Psi(d)$	Interatomic pair potential (as a function of distance, d).	[J]
Φ_s	Surface (electrical) potential	[V]
γ	Surface energy (per unit area)	[mJ/m^2]
h	Height above planar conducting surface (to where electric charge is located)	[m]
ν	Poisson's ratio	
M	Mass	[kg]
ρ	Density	[kg/m^3]
Q	Static electric charge	[C]
Q'	Image charge	[C]
Q_L	Charge located in a localized charge-patch (near the contact point)	[C]
R	Radius	[m]
R_p	Particle radius	{m]
R_{cY}	Particle radius below which plastic deformation expected with no applied load	[m]
R^*	Effective or reduced radius for two spheres of radii, R_1 and R_2; $R^*=R_1R_2/(R_1+R_2)$	
s	Gap spacing (distance between surfaces atom centers) for two near objects	[m]
s_0	Distance between surface atoms of contacting bodies at closest approach	[m]
σ	Surface charge density	[C/m^2]
V	Volume	[m^3]
$w_p(s)$	Energy per unit area as a function of separation distance, s, between two planar surfaces	[mJ/m^2]
Y	Yield strength	[GPa]

Author's short biography

Otis R. Walton

Otis Walton received his PhD in Engineering Applied Science from the University of California in 1980. While at Lawrence Livermore National Laboratory (30+ years) he specialized in modeling the properties of porous and granular materials, and developed discrete-element software to simulate the deformation and flow behavior of particulate assemblies. He spent 3 years at the University of Florida's Engineering Research Center for Particle Science, and 3 years in the pharmaceutical industry characterizing powders for pulmonary delivery of active pharmaceutical ingredients, before starting the engineering analysis and software development firm, Grainflow Dynamics, Inc. He is currently developing discrete-element simulation models for lunar regolith and also utilizing FEM codes to simulate explosions and hypervelocity impacts in geologic media. walton@grainflow.com